3-硝基邻苯二甲酸锆的制备、热分解机理及非等温反应动力学

张 衡   赵凤起*   仪建华   张晓宏   胡荣祖   徐司雨   任晓宁

(西安近代化学研究所, 西安 710065)

摘要： 用 3-硝基邻苯二甲酸、氢氧化钠和硝酸氧锆为原料, 制备了 3-硝基邻苯二甲酸锆, 采用元素分析、X 射线荧光衍射和 FT-IR 对其结构进行了表征. 用 TG-DTG 以及变温固相原位反应池/傅里叶变换红外光谱(RSFT-IR)联用技术研究了 3-硝基邻苯二甲酸锆的热分解机理, 对主分解反应的 DTG 峰进行了数学处理, 计算得到了动力学参数和动力学方程. 结果表明, 3-硝基邻苯二甲酸锆的分解反应总共有 4 个阶段, 其中主分解反应发生在第 2 阶段, 主分解反应的表观活化能 E_a 与指前因子 A 分别为 158.84 kJ·mol⁻¹ 和 $10^{9.85}$ s⁻¹, 主分解阶段的反应机理服从一级 Mample 法则, 主分解反应的动力学方程为 $d\alpha/dt=10^{9.85}(1-\alpha)e^{-1.91\times10^4/T}$.

关键词： 3-硝基邻苯二甲酸锆; 热分解机理; 非等温反应动力学

中图分类号： O643

Preparation, Thermal Behavior and Non-isothermal Decomposition Reaction Kinetics of Zr(3-NO₂-PHT)₂·2H₂O

ZHANG Heng   ZHAO Feng-Qi*   YI Jian-Hua   ZHANG Xiao-Hong

HU Rong-Zu   XU Si-Yu   REN Xiao-Ning

(*Xi'an Modern Chemistry Research Institute, Xi'an 710065, P. R. China*)

Abstract: Zirconium 3-nitrophthalate (Zr(3-NO₂-PHT)₂·2H₂O) was synthesized using 3-nitrophthalic acid, sodium hydroxide, and zirconyl nitrate as raw materials. Its structure was determined by elemental analysis, X-ray fluorescence and FT-IR spectra. The thermal decomposition mechanism and kinetic parameters of the decomposition reaction for Zr(3-NO₂-PHT)₂·2H₂O were investigated by temperature-programmed TG-DTG and condensed-phase thermolysis/FT-IR techniques. A kinetic equation for the decomposition reaction was obtained. The results showed that Zr(3-NO₂-PHT)₂·2H₂O underwent a four-stage decomposition process and that the main decomposition reaction occurred during the second process. The apparent activation energy (E_a) and pre-exponential factor (A) of the main decomposition reaction are 158.84 kJ·mol⁻¹ and $10^{9.85}$ s⁻¹, respectively. The kinetic equation can thus be expressed as: $d\alpha/dt=10^{9.85}(1-\alpha)e^{-1.91\times10^4/T}$.

Key Words: Zr(3-NO₂-PHT)₂·2H₂O; Thermal decomposition mechanism; Nonisothermal reaction kinetics

In general, aluminum powder and aluminum oxide are added in double base propellants or RDX-CMDB propellants as combustion instability inhibitors. However, much more attention has been paid on the development and research on other combustion instability inhibitors with the development of low signature propellent. Some high melting-point carbides and oxides of metals were added in double base propellants or RDX-CMDB propellants as combustion instability inhibitors by researchers[1–3]. The use of ZrC and ZrO₂ had a minimal effect on smokeless performance and fine effect on inhibiting combustion instability. However, organic zirconium compounds have not been reported. The decomposition products of organic zirconium compounds can effectively suppress combustion instability and had assistant catalysis according to our prior study[4]. In order to provide deeper insight into the mechanism of inhibiting function and catalysis, it is essential to investigate its thermal decomposition behavior

and kinetics. In this paper, a new compound $Zr(3\text{-}NO_2\text{-}PHT)_2 \cdot 2H_2O$ was prepared, its structure was determined and the thermal behavior and non-isothermal decomposition reaction kinetics were studied.

1 Experimental

1.1 Sample

All chemicals used in the synthesis were analytical-grade commercial products and were used without further purification. The title compound used in this research was prepared according to the following method: an appropriate amount of 3-nitrophthalic acid was added to the distilled water, stirred and titrated with the sodium hydroxide aqueous solution at 333 K until pH reached about 6. Then the solution of zirconyl nitrate was gradually dropped into the prepared mixture with stirring at 333 K for about 3 h, and a white precipitate was obtained. The precipitate was washed with distilled water and dried at 333 K. The title compound was obtained and kept in a vacuum desiccator before use. Element analysis (%), calcd. (found) for $Zr(3\text{-}NO_2\text{-}PHT)_2 \cdot 2H_2O$: C 35.35 (34.31), H 1.84 (2.47), N 5.15 (4.91), O 41.25 (40.90), Zr 16.41 (17.41). IR(KBr): 1718 cm^{-1} ($\nu_{-C=O}$) and 2500−4000 cm^{-1} (ν_{O-H}) vanish, 1560 cm^{-1} (ν^{as}_{-COO}), 1409 cm^{-1} (ν^{s}_{-COO}), and 3406 cm^{-1} (ν_{O-H}) appear, 1535 cm^{-1} ($\nu^{as}_{-NO_2}$) and 1351 cm^{-1} ($\nu^{s}_{-NO_2}$) do not shift. The structure of $Zr(3\text{-}NO_2\text{-}PHT)_2 \cdot 2H_2O$ is shown in Fig.1.

1.2 Equipment and conditions

TG-DTG curves under the condition of flowing nitrogen gas (purity, 99.999% ; flowing rate, 60 cm^3 ·min^{-1}; atmospheric pressure) were obtained by using a TA2950 thermal analyzer (TA Co., USA). The conditions of TG-DTG were as follows: the mass of the sample is about 1 mg; heating rates (β) were 2.5, 5, 10, and 20 K·min^{-1}.

Thermolysis/RSFT-IR measurements were conducted by using a model NEXUS 870 FT-IR spetrophptometer (Nicolet Instruments Co., USA) and situthermolysis cell (Xiamen University, China) with the temperate range of 293−723 K and the heating rate of 10 K·min^{-1}. KBr pellet samples (about 0.7 mg of $Zr(3\text{-}NO_2\text{-}PHT)_2 \cdot 2H_2O$ and 150 mg of KBr) were used. IR spectra of $ZrO(NO)_3 \cdot 2H_2O$ in the range of 4000−400 cm^{-1} were acquired by a model DTGS detector at a rate of 11 files·min^{-1} and 8 scans·file^{-1} with a resolution of 4 cm^{-1}. The main gaseous products were determined by the T-jump/FT-IR, which was used on a Nicolet 60 SXR FT-IR spectrometer equipped with an MCT-A detector.
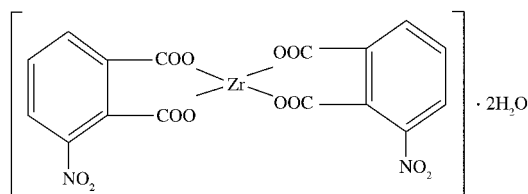
2 Results and discussion

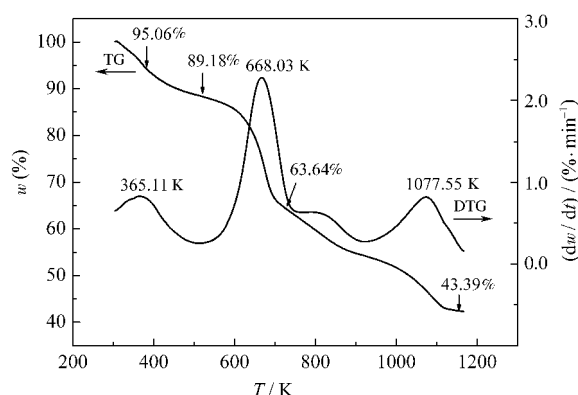Fig.1   Structure of $Zr(3\text{-}NO_2\text{-}PHT)_2 \cdot 2H_2O$

Fig.2   TG-DTG curves of $Zr(3\text{-}NO_2\text{-}PHT)_2 \cdot 2H_2O$ at a heating rate (β) of 10 K·min^{-1}

2.1 Thermal behaviors

The typical TG-DTG curves of $Zr(3\text{-}NO_2\text{-}PHT)_2 \cdot 2H_2O$ are shown in Fig.2. From Fig.2, it can be found that there are four mass loss stages in TG curve. The mass loss in the temperature range 323−373 K is attributed to the loss of adsorbent water. The first stage begins at about 373 K and stops at 473 K, accompanied with 6.39% mass loss, which is in agreement with the theoretical value of the mass loss of 6.63%, corresponding to the mass of $2H_2O$. The second stage begins at 523 K and stops at 723 K, accompanied with 25.54% mass loss. It is in agreement with the theoretical value of the mass loss of 24.69% and the residue amounts are $ZrOCO_3$[5] and carbon. The third and forth stages in the temperature range 723−1173 K are attributed to the decomposition of $ZrOCO_3$ and the oxidation of a few of carbon. At the end of decomposition process, the residue amounts to 43.39% (ZrO_2+C). Additionly, from the DTG curves of $Zr(3\text{-}NO_2\text{-}PHT)_2 \cdot 2H_2O$ at different heating rates as shown in Fig.3, we can seen that the peak temperature of DTG curve augments with the increase of the heating rate.

The IR spectra and characteristic absorption peak intensities of the condensed phase decomposition products of $Zr(3\text{-}NO_2\text{-}PHT)_2 \cdot 2H_2O$ at different temperatures are shown in Figs.4 and 5, respectively. From Figs.4 and 5, one can find that the intensity of the 3406 cm^{-1} (ν_{O-H}) weaken rapidly at 473.2 K and the intensity of
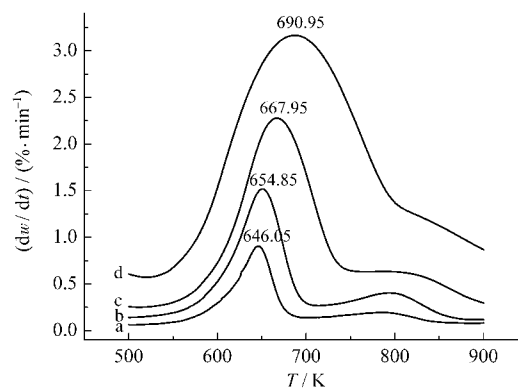

Fig.3   DTG curves of $Zr(3\text{-}NO_2\text{-}PHT)_2 \cdot 2H_2O$ at different heating rates

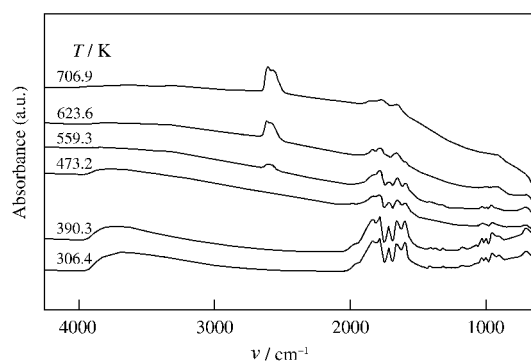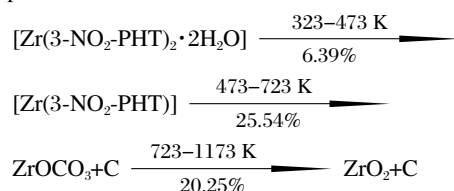β/(K·min^{-1}): a) 2.5; b) 5; c) 10; d) 20

Fig.4   IR spectra of the condensed phase decomposition products of Zr(3-NO$_2$-PHT)$_2$·2H$_2$O at various temperatures

the 1560 cm^{-1} (ν^{as}_{-COO}), 1409 cm^{-1} (ν^{s}_{-COO}), 1535 cm^{-1} ($\nu^{as}_{-NO_2}$), and 1351 cm^{-1} ($\nu^{s}_{-NO_2}$) weaken rapidly in the temperature range of 473.2−623.6 K. This indicates that the main decomposition process of compound and the break of C—NO$_2$ bond occur in the second stage. In addition, the intensity of the 1480 cm^{-1} ($\nu_{CO_3^{2-}}$) strengthens rapidly in the temperature range 473.2−706.9 K because of the appearance of ZrOCO$_3$[6–8].

On the basis of above-mentioned experimental results, the thermal decomposition mechanism of Zr(3-NO$_2$-PHT)$_2$·2H$_2$O can be expressed as:

$$[Zr(3\text{-}NO_2\text{-}PHT)_2 \cdot 2H_2O] \xrightarrow[6.39\%]{323–473\ K}$$

$$[Zr(3\text{-}NO_2\text{-}PHT)] \xrightarrow[25.54\%]{473–723\ K}$$

$$ZrOCO_3 + C \xrightarrow[20.25\%]{723–1173\ K} ZrO_2 + C$$

2.2   Non-isothermal calculation kinetics

In order to obtain the most probable mechanism function and the corresponding kinetic parameters for the main decomposition process of the compound, three integral methods and three differential methods listed in Table 1 are employed[9–20].

The values of activation energy (E_a) were obtained by intergral isoconversional nonlinear method with conversion degree (α) changing from 0.02 to 1.00 and the E_a−α relation is shown in

Table 1   Kinetic analysis methods and corresponding equations[9–20]

Method	Equation	
general integral	$\ln[G(\alpha)/T^2]=\ln[AR/\beta E](1-2RT/E)]-E/RT$	(1)
Šatava-Šesták	$\lg[G(\alpha)]=\lg[A_S E_S/\beta R]-2.315-0.4567E_S/RT$	(2)
Flynn-Wall-Ozawa	$\lg\beta=\lg\{AE/[RG(\alpha)]\}-2.315-0.4567E/RT$	(3)
Achar-Brindley	$\ln\{d\alpha/[f(\alpha)dT]\}=\ln A/\beta-E_a/RT$	(4)
differential equation	$\ln\{(d\alpha/dT)/[f(\alpha)[E(T-T_0)/RT^2+1]]\}=\ln(A/\beta)-E/R$	(5)
Kissinger	$\ln(\beta/T_{pi}^2)=\ln(A_k R/E_k)-E_k/RT_{pi}$ (i=1, 2, 3, 4)	(6)

α is fractional decomposition, T is temperature (K) at time t, T_0 is the initial point at which DTG curve deviates from the baseline, R is the gas constant, A is the pre-exponential factor, E is the apparent activation energy, β is the heating rate, $f(\alpha)$ and $G(\alpha)$ are the differential and integral mechanism functions, respectively, T_p is the peak temperature of DTG curve. The data need for the equations of the intergral and differential methods, i, α_i, β, T_i, T_p, $(d\alpha/dT)_i$ (i=1, 2, 3,···, 50), are obtained from the DTG curves and summarized in Table 2.

Fig.6. It indicates that the activation energy of the decomposition process changes greatly by diverse level with an increase in the conversion degree, except for the section of α=0.04−0.98, in which activation energy changes faintly, and it means that the decomposition mechanism of the process does not involve transference in essence, or the transference can be ignored. Therefore, it is feasible to research into the reaction mechanism and kinetics in the section of α=0.04−0.98.

Forty-one types of kinetic model functions in Ref.[9] and the original data tabulated in Table 2 were put into Eqs.(1)−(6), respectively, for calculations. The values of E_a, $\lg A$, linear correlation coefficient (r), and standard mean square deviation (Q) can be calculated on the computer with linear least-squares method at various heating rates of 2.5, 5, 10, 20 K·min^{-1}. The most probable mechanism function is selected by the better values of r and Q taken from Ref.[9]. The results of satisfying the conditions mentioned above are listed in Table 3.

The values of E_a and $\lg A$ obtained from a single non-isothermal DTG curve are in approximately good agreement with the values calculated by Kissinger's method and Flynn-Wall-Ozawa's method. Therefore, a conclusion can be drawn that the reaction mecha -nism of the main decomposition process of Zr(3-NO$_2$-PHT)$_2$·2H$_2$O is controlled by Mample Law (n=1). Substituting f
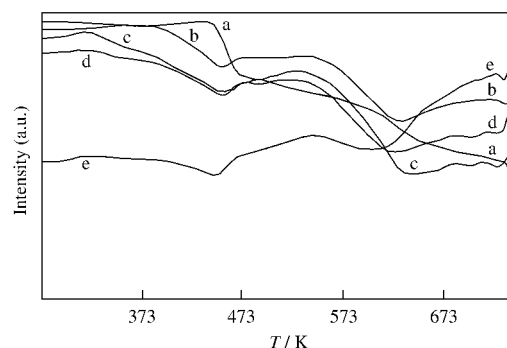

Fig.5   IR characteristic absorption peak intensity of the condensed phase decomposition products of Zr(3-NO$_2$-PHT)$_2$·2H$_2$O at different frequencies

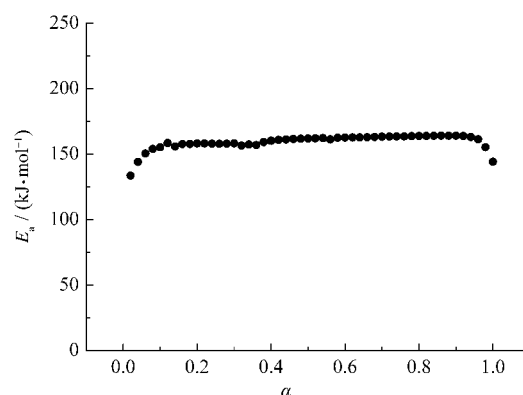ν/cm^{-1}: a) 3406, b) 1409, c) 1535, d) 1351, e) 1480

Fig.6 E_a−α curve obtained by intergral isoconversional non-linear method

Table 2　Basic data for the main decomposition process of Zr(3-NO$_2$-PHT)$_2$·2H$_2$O

α	β=2.5 K·min^{-1}		β=5 K·min^{-1}		β=10 K·min^{-1}		β=20 K·min^{-1}	
	T/K	$10^3(\mathrm{d}\alpha/\mathrm{d}T)$/K^{-1}	T/K	$10^3(\mathrm{d}\alpha/\mathrm{d}T)$/K^{-1}	T/K	$10^3(\mathrm{d}\alpha/\mathrm{d}T)$/K^{-1}	T/K	$10^3(\mathrm{d}\alpha/\mathrm{d}T)$/K^{-1}
0.02	572.23	1.85	579.71	1.69	603.52	2.30	607.46	1.65
0.04	583.05	2.33	591.53	2.07	612.22	2.79	619.57	2.10
0.06	590.16	3.22	599.72	2.90	618.32	3.69	627.41	2.93
0.08	595.66	4.10	605.69	3.85	623.20	4.45	633.47	3.66
0.10	600.05	4.57	610.29	4.75	627.36	5.12	638.44	4.39
0.12	604.41	6.43	614.17	5.51	631.04	5.76	642.64	5.09
0.14	606.83	7.17	617.58	6.16	634.33	6.36	646.33	5.76
0.16	610.12	6.93	620.68	6.77	637.34	6.97	649.61	6.38
0.18	612.69	7.86	623.50	7.39	640.08	7.54	652.61	6.89
0.20	615.21	8.43	626.10	7.94	642.65	8.08	655.42	7.36
0.22	617.45	9.39	628.54	8.54	645.04	8.65	658.05	7.93
0.24	619.48	10.13	630.79	9.18	647.28	9.25	660.47	8.56
0.26	621.40	10.67	632.90	9.87	649.37	9.89	662.73	9.19
0.28	623.23	11.15	634.85	10.53	651.33	10.51	664.83	9.86
0.30	624.99	14.02	636.70	11.15	653.18	11.22	666.79	10.51
0.32	626.19	20.68	638.44	11.81	654.90	11.91	668.64	11.09
0.34	627.00	16.93	640.09	12.47	656.54	12.51	670.40	11.63
0.36	629.18	9.61	641.65	13.12	658.10	13.17	672.08	12.24
0.38	631.17	11.24	643.14	13.75	659.58	13.85	673.67	12.87
0.40	632.78	13.25	644.56	14.40	660.99	14.45	675.19	13.43
0.42	634.20	14.62	645.92	15.05	662.35	14.99	676.65	14.04
0.44	635.52	15.51	647.22	15.63	663.66	15.57	678.04	14.66
0.46	636.78	16.41	648.48	16.13	664.92	16.13	679.38	15.15
0.48	637.96	17.32	649.70	16.67	666.14	16.74	680.68	15.69
0.50	639.09	18.11	650.88	17.25	667.31	17.24	681.93	16.20
0.52	640.17	18.69	652.02	17.70	668.46	17.55	683.15	16.60
0.54	641.23	19.14	653.14	18.10	669.59	17.94	684.34	17.02
0.56	642.26	19.42	654.23	18.52	670.69	18.35	685.50	17.47
0.58	643.29	19.61	655.30	18.78	671.77	18.61	686.63	17.78
0.60	644.30	19.90	656.36	19.05	672.84	18.78	687.75	17.94
0.62	645.30	20.20	657.40	19.32	673.90	18.87	688.86	18.10
0.64	646.28	20.31	658.43	19.32	674.96	18.87	689.96	18.27
0.66	647.27	20.10	659.47	19.32	676.02	18.87	691.05	18.27
0.68	648.27	19.90	660.50	19.32	677.08	18.78	692.15	18.10
0.70	649.28	19.80	661.54	19.05	678.15	18.52	693.26	17.86
0.72	650.29	19.61	662.60	18.78	679.24	18.18	694.39	17.62
0.74	651.32	19.14	663.67	18.44	680.35	17.70	695.53	17.25
0.76	652.38	18.61	664.77	17.94	681.50	17.17	696.71	16.81
0.78	653.47	18.02	665.90	17.32	682.68	16.54	697.91	16.27
0.80	654.60	17.25	667.08	16.67	683.92	15.64	699.17	15.57
0.82	655.79	16.22	668.30	15.83	685.24	14.67	700.48	14.78
0.84	657.07	15.06	669.61	14.78	686.65	13.54	701.88	13.77
0.86	658.45	13.87	671.01	13.64	688.20	12.30	703.39	12.61
0.88	659.96	12.47	672.55	12.31	689.91	11.03	705.06	11.25
0.90	661.67	10.80	674.27	10.89	691.84	9.51	706.96	9.65
0.92	663.69	9.02	676.24	9.24	694.15	7.78	709.24	7.91
0.94	666.15	7.08	678.64	7.32	697.05	5.89	712.08	6.02
0.96	669.47	4.85	681.81	5.15	701.15	3.77	716.08	3.89
0.98	674.90	2.29	686.83	2.30	708.68	1.64	723.25	1.72
1.00	697.35	0.89	719.35	0.62	741.15	0.62	753.75	0.66
	T_p=646.05 K		T_p=654.85 K		T_p=667.95 K		T_p=690.95 K	

$(\alpha)(=1-\alpha)$, $E_a(=158.84$ kJ·mol^{-1}), and $A(=10^{9.85}$ s^{-1}) into Eq.(7):

$$\mathrm{d}\alpha/\mathrm{d}t = Af(\alpha)\mathrm{e}^{-E_a/RT} \qquad (7)$$

And the kinetic equation of the main decomposition reaction of [Zr(3-NO$_2$-PHT)(H$_2$O)$_2$] may be described as:

Table 3   Kinetic parameters obtained for the main decomposition process of Zr(3-NO$_2$-PHT)$_2$·2H$_2$O

Method	β/(K·min^{-1})	E_a/(kJ·mol^{-1})	lg(A/s^{-1})	r	Q
general integrate	2.5	153.81	9.75	0.9988	0.1114
	5	153.12	9.75	0.9982	0.1708
	10	161.86	10.42	0.9991	0.0866
	20	156.52	10.02	0.9984	0.1495
Šatava-Šesták	2.5	156.21	9.58	0.9989	0.0219
	5	155.72	9.98	0.9984	0.0336
	10	164.33	10.63	0.9992	0.0165
	20	159.44	10.27	0.9986	0.0294
Achar-Brindley	2.5	157.79	10.09	0.9887	1.1516
	5	162.24	10.49	0.9946	0.5793
	10	156.22	9.97	0.9866	1.2100
	20	161.21	10.38	0.9896	1.0559
differential equation	2.5	158.93	8.92	0.9888	1.1520
	5	163.52	9.33	0.9946	0.5831
	10	157.72	8.84	0.9869	1.2068
	20	162.85	9.25	0.9898	1.0561
mean		158.84	9.85		
Kissinger		163.09	10.48	0.9994	0.0025
Flynn-Wall-Ozawa		165.65		0.9995	0.0005

r: linear correlation coefficient, Q: standard mean square deviation

$$d\alpha/dt = 10^{9.85}(1-\alpha)e^{-1.91\times10^4/T} \tag{8}$$

3   Conclusions

(1) Zr(3-NO$_2$-PHT)$_2$·2H$_2$O was synthesized and the structure was determined.

(2) The decomposition process of Zr(3-NO$_2$-PHT)$_2$·2H$_2$O had four stages and the main decomposition reaction occurred in the second stage. The mechanism of the thermal decomposition reaction of the compound was obtained.

(3) The kinetics of the main decomposition reaction of Zr(3-NO$_2$-PHT)$_2$·2H$_2$O was investigated, and the kinetic model function in differential form, apparent activation energy, and pre-exponential constant of this reaction was $1-\alpha$, 158.84 kJ·mol^{-1}, and $10^{9.85}$ s^{-1}, respectively.

References

1   Dobbins, R. A.; Providence, R. I. Method for minimizing combustion instability. US Patent, 3310964. 1967

2   Cohen, J.; Zimmerman, G. A. Solid propellants with stability enhanced additives of particulate refractory carbides or oxides. US Patent, 3924405. 1975

3   Zhang, H.; Zhang, X. H.; Zhao, F. Q. *Winged Missiles J.,* **2008, 7**: 50   [张　衡, 张晓宏, 赵凤起. 飞航导弹, **2008, 7**: 50]

4   Zhao, F. Q. Master Dissertation. Xi'an: Xi'an Modern Chemistry Research Institute, 1986   [赵凤起. 硕士学位论文. 西安: 西安近代化学研究所, 1986]

5   Luo, F. C.; Lü, W. G.; Luo, X. W. *Chin. J. Rare Metals,* **2003, 27**: 53   [罗方承, 吕文广, 罗新文. 稀土金属, **2003, 27**: 53]

6   Li, J. Z.; Zhang, G. F.; Fan, X. Z.; Hu, R. Z.; Pan, Q. J. *Anal. Appl. Pyrolysis,* **2007, 76**: 1

7   Yi, J. H.; Zhao, F. Q.; Gao, H. X.; Xu, S. Y.; Hu, R. Z.; Wang, Y. *Chin. J. Expls. Propellants,* **2007, 30**: 1   [仪建华, 赵凤起, 高红旭, 徐司雨, 胡荣祖, 汪　渊. 火炸药学报, **2007, 30**: 1]

8   Song, X. D.; Zhao, F. Q.; Liu, Z. R.; Pan, Q.; Luo, Y. *Chem. J. Chin. Univ.,* **2006, 27**: 125   [宋秀铎, 赵凤起, 刘子如, 潘　清, 罗　阳. 高等学校化学学报, **2006, 27**: 125]

9   Hu, R. Z.; Gao, S. L.; Zhao, F. Q.; Shi, Q. Z.; Zhang, T. L.; Zhang, J. J. Thermal analysis kinetics. 2nd ed. Beijing: Science Press, 2008: 54   [胡荣祖, 高胜利, 赵凤起, 史启祯, 张同来, 张建军. 热分析动力学. 第二版. 北京: 科学出版社, 2008: 54]

10   Zhao, F. Q.; Hu, R. Z.; Gao, H. X.; Ma, H. X. In: New developments in hazardous materials research. Bronna, O. E. Ed. New York: Nova Science Publishers, Inc., 2006, Chapter 4: 93

11   Yi, J. H.; Zhao, F. Q.; Xu, S. Y.; Gao, H. X.; Hu, R. Z.; Hao, H. X.; Pei, Q.; Gao, Y. *Acta Phys. -Chim. Sin.,* **2007, 23**: 1316   [仪建华, 赵凤起, 徐司雨, 高红旭, 胡荣祖, 郝海霞, 裴　庆, 高　茵. 物理化学学报, **2007, 23**: 1316]

12   Xu, K. Z.; Ma, H. X.; Song, J. R.; Huang, J.; Ren, Y. H.; Hu, R. Z. *J. Chin. Chem. Soc.,* **2007, 54**: 277   [徐抗震, 马海霞, 宋纪荣, 黄　洁, 任莹辉, 胡荣祖. 中国化学会会志, **2007, 5**4: 277]

13   Zhao, F. Q.; Hu, R. Z.; Gao, H. X.; Ma, H. X. *J. Chin. Ordnance,* **2007, 3**: 68

14   Hu, R. Z.; Chen, S. P.; Gao, S. L.; Zhao, F. Q.; Luo, Y.; Gao, H. X.; Shi, Q. Z.; Zhao, H. A.; Yao, P.; Li, J. *J. Hazard. Mater.,* **2005, 117**: 103

15   Song, J. R.; Ma, H. X.; Huang, J.; Hu, R. Z.; Kang, B. *J. Chin. Chem. Soc.,* **2005, 52**: 1089   [宋纪荣, 马海霞, 黄　洁, 胡荣祖, 康　冰. 中国化学会会志, **2005, 52**: 1089]

16   Gao, H. X.; Zhao, F. Q.; Hu, R. Z.; Pan, Q.; Wang, B. Z.; Yang, X. W.; Gao, Y.; Gao, S. L.; Shi, Q. Z. *Chin. J. Chem.,* **2006, 24**: 177

17   Jiao, B. J.; Chen, S. P.; Zhao, F. Q.; Hu, R. Z.; Gao, S. L. *J. Hazard. Mater.,* **2007, 142**: 550

18   Ma, H. X.; Song, J. R.; Zhao, F. Q.; Hu, R. Z.; Xiao, H. M. *J. Phys. Chem. A,* **2007, 111**: 8642

19   Ma, H. X.; Song, J. R.; Xiao, H. M.; Hu, R. Z.; Wang, H. L.; Jin, P. J.; Wang, Y. *J. Hazard. Mater.,* **2006, 128**: 116

20   Guo, P. J.; Jiao, B. J.; Chen, S. P.; Hu, R. Z.; Gao, S. L.; Shi, Q. Z. *Sci. China Ser. B,* **2005, 48**: 83   [郭鹏江, 焦宝娟, 陈三平, 胡荣祖, 高胜利, 史启祯. 中国科学 B 辑, **2005, 48**: 83]